Journal of Computational Neuroscience 7, 5–15 (1999)

Role of an A-Type K^+ Conductance in the Back-Propagation of Action Potentials in the Dendrites of Hippocampal Pyramidal Neurons

M. MIGLIORE
National Research Council, Institute of Advanced Diagnostic Methodologies, Palermo, Italy
migliore@iaif.pa.cnr.it

D.A. HOFFMAN*
Division of Neuroscience, Baylor College of Medicine, Houston, TX 77030

J.C. MAGEE
Neuroscience Center, Louisiana State University Medical Center, New Orleans, LA 70112

D. JOHNSTON
Division of Neuroscience, Baylor College of Medicine, Houston, TX 77030

Received ; Revised ; Accepted

Action Editor: Roger Traub

Abstract. Action potentials elicited in the axon actively back-propagate into the dendritic tree. During this process their amplitudes can be modulated by internal and external factors. We used a compartmental model of a hippocampal CA1 pyramidal neuron to illustrate how this modulation could depend on (1) the properties of an A-type K^+ conductance that is expressed at high density in hippocampal dendrites and (2) the relative timing of synaptic activation. The simulations suggest that the time relationship between pre- and postsynaptic activity could help regulate the amplitude of back-propagating action potentials, especially in the distal portion of the dendritic tree.

Keywords: computational model, action potential, back propagation, K_A conductance, associative interactions

Introduction

The generation of an action potential (AP) and its propagation through the neuron play a fundamental role in determining how external inputs are processed by the dendritic tree (Jefferys, 1975; Zador et al., 1990). For example, the temporal overlap of pre- and postsynaptic events results in a local amplification of the amplitude of a back-propagating AP and local Ca^{2+} influx (Magee and Johnston, 1997; Schiller et al., 1998; Koester and Sakmann, 1998) with possible consequences for the induction of short- or long-term modifications of synaptic strength. The coincidence of an AP with a synaptic input has been shown experimentally (Debanne et al., 1998; Magee and Johnston, 1997; Markram et al., 1997; Bi and Poo, 1998) to be an important step in establishing an associative interaction between two inputs provided one input triggers an AP in the postsynaptic neuron. A transient, A-type K^+ conductance, which is expressed at a high density in hippocampal

*Current address: Max-Planck-Institut fur Medizimische Forschung, Jahnsbrasse 29, D69120 Heidelberg, Germany.

dendrites, has been suggested to participate in this process (Hoffman et al., 1997). Briefly, excitatory synaptic input could inactivate this K^+ conductance, leading to an enhancement in the amplitude of back-propagating APs and related Ca^{2+} influx in the local vicinity of the synapse. This process could help establish an associative coupling between a strong (suprathreshold) and a weak (subthreshold) synaptic input. To understand how this mechanism could be effectively used as a Hebbian learning rule, the relevant mechanisms and their interplay in the modulation of the back-propagation of an AP must be investigated. We will show here, using a compartmental model of a hippocampal CA1 pyramidal neuron, how the amplitude of a back-propagating AP could be modulated by internal factors, such as the local properties of the voltage-gated channels, as well as by external factors, such as the timing of synaptic activation.

Methods

Computational Details

We performed our simulations with the program NEURON (version 4.0.1) (Hines and Carnevale, 1997) on a DEC Alphaserver 4100 5/400 workstation, using a 10 μs time step. A reconstructed hippocampal CA1 pyramidal cell (Fig. 1A, courtesy of D. Turner) was modeled with NEURON using a total of 202 compartments for the axon, soma, and dendrites. Where necessary, each compartment was further subdivided in smaller segments not longer than 0.1λ. An intracellular resistivity of $R_a = 150\ \Omega$ cm ($R_a = 50\ \Omega$ cm in the axon), a membrane time constant of $\tau_m = 28$ ms ($R_m = 28$ kΩ cm^2, and $C_m = 1\ \mu$F/cm^2), and a membrane resting potential of $V_{\text{rest}} = -65$ mV were used. To account for spines and smaller dendritic branches that were not explicitly modeled, C_m was increased and R_m decreased (Holmes, 1986) by a factor of 2 in the apical dendrites. An input resistance of $R_N \simeq 129\,\text{M}\Omega$ resulted from our model.

Channel Kinetics

We have chosen to limit the set of voltage-dependent conductances to those strictly needed to shape an AP and to model the set of experimental data that we used as a starting point (Hoffman et al., 1997). For this reason, only a Na^+ (g_{Na}) and two K^+ (g_{KDR} and g_{K_A}) conductances were inserted in the axon, the soma, and all the basal or apical compartments with a diameter bigger than 0.5 μm and up to 500 μm from the soma. The remaining compartments were considered passive. The voltage-dependence of the steady-state activation and inactivation curves and their time constants are shown in Fig. 2. The expressions for the kinetics are reported in the APPENDIX, and the NEURON model files are available from one of the authors (MM). Excitatory synaptic conductances were inserted in active compartments of the main apical dendritic shaft at 200, 250, and 400 μm from the soma and modeled as simple α-functions, using the built-in NEURON point process *AlphaSynapse()* with time constants and reversal potential of $\tau_{\text{esyn}} = 3$ ms and $e_{\text{erev}} = 0$.

g_{Na} Conductance

Our model for this conductance is consistent with several experimental constraints showing that

- The soma must be able to actively generate a full amplitude AP when Na^+ channels in the axon are pharmacologically blocked (Colbert and Johnston, 1996);
- The Na^+ channel density and kinetic properties should be similar in the soma and apical dendrites (Magee and Johnston, 1995);
- A full-amplitude AP should be actively generated in the dendrites when most of the K^+ conductances are pharmacologically blocked (Hoffman et al., 1997);
- The site of AP initiation is in the axon, where the membrane potential threshold for orthodromic spikes appears to be lower than in the soma, as suggested by simultaneous somatic and axonal recordings from neocortical neurons (Stuart and Sakmann, 1994) and cerebellar Purkinje cells (Stuart and Häusser, 1992), as well as simultaneous recordings from the soma and the initial segment of subicular pyramidal neurons (Colbert and Johnston, 1996).

The latter experimental evidence suggested that the properties of the Na^+ channels in the axon must be different, in density or in the activation properties, from those in the soma and in the dendrites. Different values have been proposed (Mainen et al., 1995; Rapp et al., 1996). We found that with our model, a two-fold increase in the peak conductance in the axon was sufficient to be consistent with the experimental findings. The same peak conductance density ($\bar{g}_{\text{Na}} = 32$ mS/cm^2) was used for the soma and all the active compartments. For the activation curve we

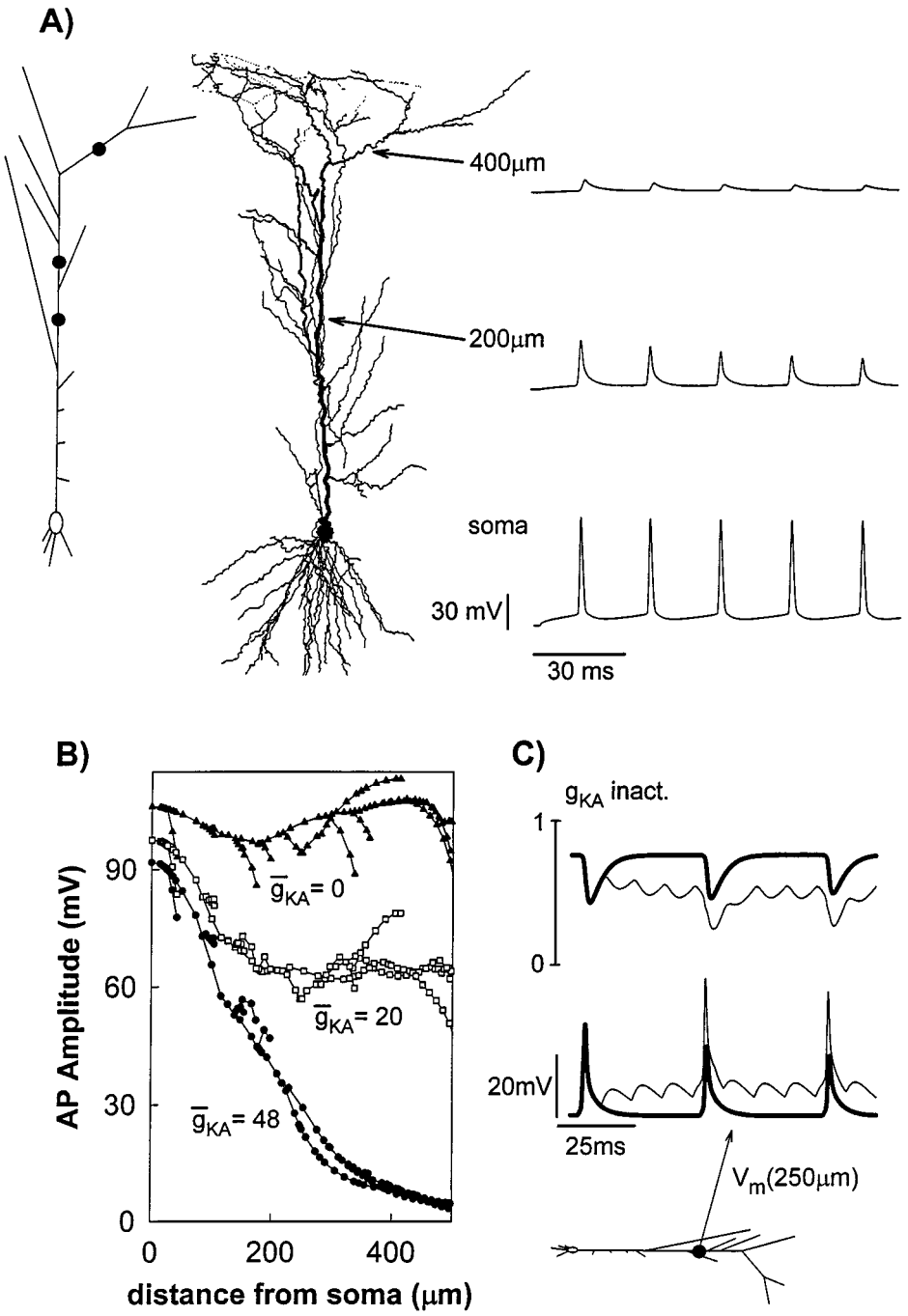

Figure 1. A: Control simulation in which a 0.15 nA current step was delivered at the soma. Membrane potential is shown at the soma and at two dendritic locations. The diagram on the left shows a schematic representation of the active compartments and the locations used for synaptic input at 200, 250, and 400 μm from the soma (black symbols). B: Distribution of the peak membrane depolarization, as a function of the distance from soma, in response to a single AP elicited by a short somatic current pulse (1 nA, 1.2 ms) using different values for the peak g_{K_A} conductance (in mS/cm^2) at the soma. C: Effects of pairing synaptic stimulation with back-propagating action potentials. Membrane potential (lower traces) and the gating variable for g_{K_A} inactivation (upper traces) are shown at the site of synaptic stimulation. A train of action potentials was elicited at 25 Hz by short current pulses at the soma (1 nA, 1.2 ms) with (light lines) or without (heavy lines) a 100 Hz synaptic stimulation ($\bar{g}_{\text{esyn}} = 4$ nS) delivered at 250 μm from the soma, where indicated in the schematic diagram at the bottom.

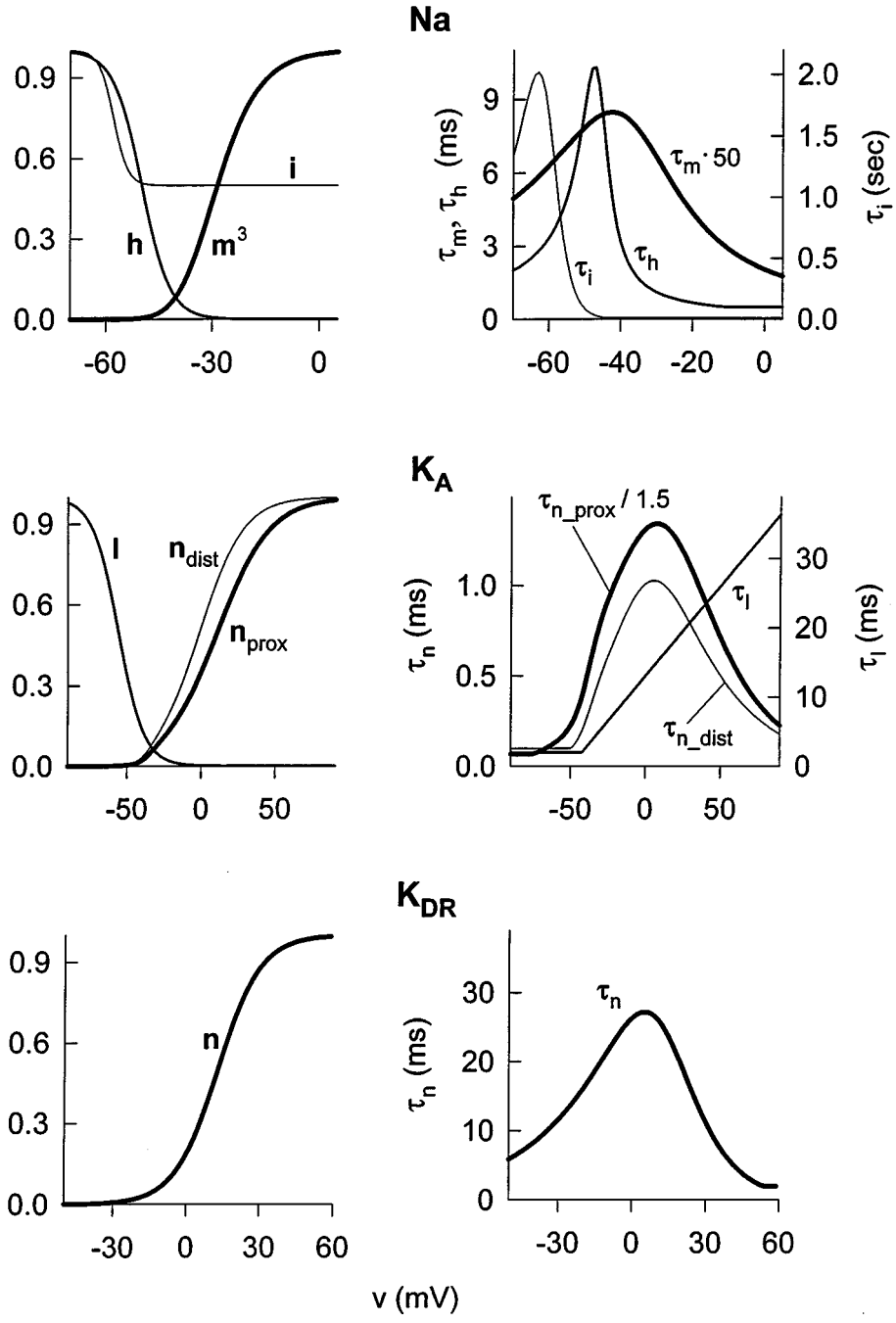

Figure 2. Voltage-dependence of the steady-state and time constants for the activation and inactivation curves of the conductances used in the model.

used the parameters derived from patch clamp recordings of Na^+ channels in hippocampal CA1 pyramidal neurons (Magee and Johnston, 1995). However, we had to modify the parameters for the inactivation kinetic. In fact, using the values derived from the voltage-clamp experiments, under a somatic current injection (current-clamp) the channel undergoes a significant inactivation. This is in contrast to the experiments showing that a full-amplitude AP is generated in the soma even from a depolarized membrane potential (∼15 mV from rest, Colbert and Johnston, 1996). We found that a +12 mV shift in the $V_{1/2}$ of

inactivation (from -62 to -50) and a decrease in the shape factor (from 6.9 to 4) gave a reasonable agreement with both voltage- and current-clamp experiments. An additional gate variable (Migliore, 1996) was included to account for the slow inactivation of dendritic Na^+ channels experimentally observed in hippocampal CA1 pyramidal neurons (Colbert et al., 1997; Jung et al., 1997). This slow inactivation has been experimentally shown to be small at the soma and rather high in dendritic patches at $\sim$200 μm, and the maximum effect was shown to be dependent on protein kinase C activation (Colbert and Johnston, 1998; Mickus et al., 1999). Thus, a nonuniform distribution could be expected for this property throughout the neuron, according to (perhaps) the local phosphorylation activity. We have chosen to limit to half-maximum its activation in the apical dendrites (i.e., $b_i = 0.5$, see the Appendix) and to 20% of maximum ($b_i = 0.8$) in the soma. No slow inactivation was included in the basal dendrites.

g_{K_A} *Conductance*

The distribution and the kinetic properties that we used for our model of this conductance were consistent with the experimental findings in CA1 hippocampal neurons (Hoffman et al., 1997). In those experiments application of 4-aminopyridine (4-AP) into the bath resulted in the AP back-propagating into the dendrites essentially without attenuation, suggesting that an AP is usually clipped by a strong A-type K^+ conductance that reduces the AP amplitude to $\sim$30 mV at $\sim$250 μm from the soma. The same experiments suggested a linear increase in the g_{K_A} channel density with distance from the soma and different voltage ranges of activation between channels located in the soma and distal dendrites. We used two A-type K^+ conductances, $g_{K_A(prox)}$ for the soma, basal dendrites, and apical dendrites less than 100 μm from the soma, and $g_{K_A(dist)}$ for the apical dendrites more than 100 μm from the soma. In agreement with experimental findings on soma- and dendrite-attached patches (Hoffman et al., 1997), the activation curve of $g_{K_A(dist)}$ was shifted by -12 mV, with respect to $g_{K_A(prox)}$, and the time constant of inactivation τ_l was increased linearly with voltage. A $\bar{g}_{K_A} = 48$ mS/cm^2 was used as peak value at the soma, linearly increasing with $(d/100)$, where d was the distance from soma (in μm).

$g_{K_{DR}}$ *Conductance*

We based our model for this noninactivating K^+ conductance on the experimental findings in hippocampal CA1 pyramidal neurons (Hoffman et al., 1997). Its distribution follows g_{Na}, and a uniform peak density of $\bar{g}_{K_{DR}} = 10$ mS/cm^2 was used for all the involved compartments. It had a major role in setting the interspike interval under a constant current injection and in shaping the late repolarization phase of an AP.

Results

In Fig. 1A we illustrate the model neuron, a schematic diagram showing the active compartments and the locations we used for synaptic input (black symbols) and a control simulation (0.15 nA somatic current injection for 100 ms). The amplitude of the AP was reduced with distance from the soma by the repolarizing action of the g_{K_A} conductance. The specific properties of the membrane, such as the channel density or phosphorylation activity, will help determine AP amplitude (Hoffman and Johnston, 1998). This is illustrated in Fig. 1B, where we show the distribution of the peak value of the membrane potential, reached during a single back-propagating AP, as a function of the distance from soma using different values of $\bar{g}_{K_A}$.

How is the amplitude of an AP modified if a synaptic input is active at a given location at the time when a back-propagated AP arrives? Experiments (Magee and Johnston, 1997; Hoffman et al., 1997) have shown that an increase in the amplitude of the AP in the dendrites occurs when the AP is paired with synaptic activation in the distal dendrite. This supralinear increase in AP amplitude was suggested to occur because of inactivation of the g_{K_A} conductance by the synaptic input. In a simulation, Fig. 1C, a series of APs were elicited at 25 Hz with short current pulses at the soma. In the absence of any synaptic input, the amplitudes of the APs observed at 250 μm from the soma (Fig. 1C, heavy lines) were $\sim$30 mV and the inactivation variable for the g_{K_A} conductance l relaxed to its steady-state value at the resting potential after each somatic stimulation. When a local synaptic input (4 nS, 100 Hz) was paired with the back-propagating APs (Fig. 1C, light lines), the depolarization induced by the synaptic activity inactivated the g_{K_A} conductance, reducing the repolarizing current and, thus, increasing the amplitude of the AP and reproducing the experimental observations.

Effects of Pairing an AP with a Synaptic Input at Different Time Intervals

A necessary condition for Hebbian synaptic plasticity is that the signals involved in the associative

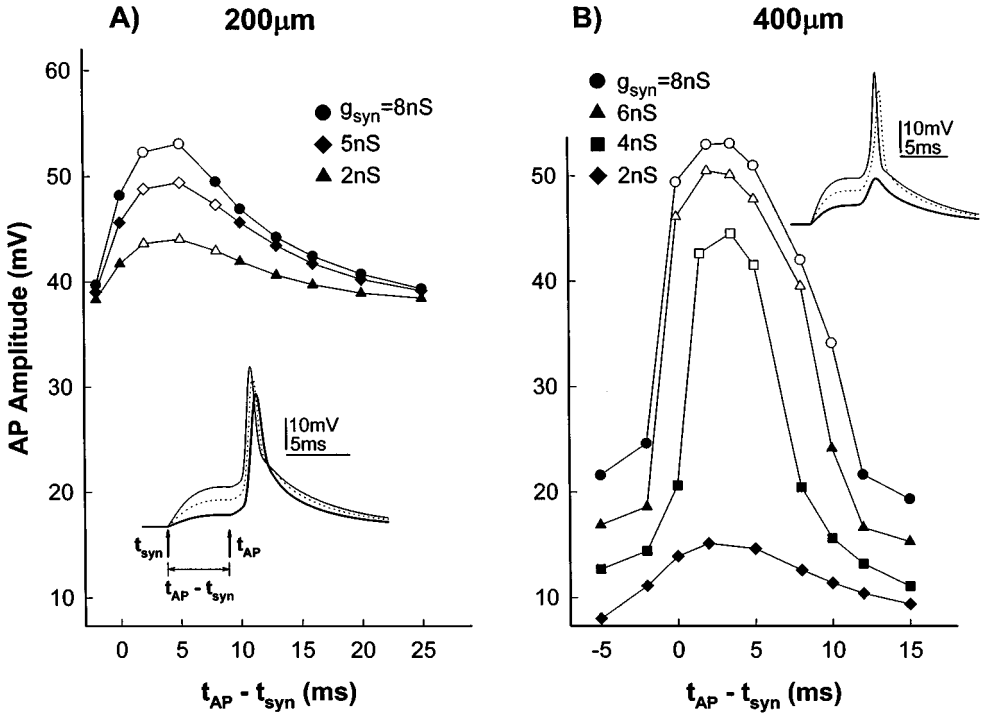

Figure 3. AP amplitude after pairing a synaptic input (delivered at $t = t_{\rm syn}$) with an AP (elicited at the soma at $t = t_{\rm AP}$) using different time delays, $t_{\rm AP} - t_{\rm syn}$, and different values of $\bar{g}_{\rm syn}$. A: Synaptic input at 200 μm from soma; the inset shows the membrane potential at the site of synaptic stimulation for $t_{\rm AP} - t_{\rm syn} = 5$ ms and $\bar{g}_{\rm syn} = \{2,5,8\}$ nS. B: Synaptic input at 400 μm from soma; the inset shows the membrane potential at the site of synaptic stimulation for $t_{\rm AP} - t_{\rm syn} = 3.5$ ms and $\bar{g}_{\rm syn} = \{2,4,6\}$ nS. In both panels, open symbols indicate the region of supralinear amplification, and closed symbols sublinear summation. Linear summation occurs between the two sets of symbols.

interaction occur within a given window of time (Bekkers and Stevens, 1990; Gustafsson et al., 1989). This coincidence mechanism has been experimentally found at different levels of integration, from synaptic populations targeting large receptive dendritic fields (Barrionuevo and Brown, 1983; Kelso and Brown, 1986; Levy and Steward, 1983) to more localized synaptic sites (Debanne et al., 1998; Magee and Johnston, 1997; Markram et al., 1997; Bi and Poo, 1998). Because of its unique kinetic characteristics and its distribution on the neural membrane, the K_A current could play a role in setting these timing constraints. We addressed this issue using a subthreshold synaptic input paired with a back-propagating AP. A synaptic input was delivered at either of two different compartments (200 or 400 μm from the soma) and paired with an AP elicited at the soma with different time delays. The results, summarized in Fig. 3, showed that for the more proximal synaptic input (Fig. 3A, 200 μm), the effect of pairing was a small supralinear superposition when the AP was elicited 2 to 8 ms after the synaptic activation (Fig. 3, open symbols) and sublinear outside this range (closed symbols). A much stronger amplification was obtained for more distal inputs (Fig. 3B, 400 μm) for sufficiently strong inputs activated 2 to 8 ms before the AP. It could be expected that if this time window depends on the kinetic characteristics of the K_A current, then it might be modulated by the local phosphorylation activity. As an example, we illustrate in Fig. 4 how a change in the inactivation time constant altered the interaction between an AP and a synaptic input ($\bar{g}_{\rm syn} = 4$ nS) in the distal dendrite. In Fig. 4A, the time constant of $g_{\rm K_A(dist)}$ inactivation τ_l was increased or decreased by a factor of 1.5. This resulted in a significant change in the characteristics of the time window. In particular, an increase of τ_l resulted in essentially no amplification of the AP, whereas a decrease caused a supralinear amplification and a larger time window. The membrane potential at 400 μm is shown in Fig. 4B for the paired activation of a synaptic input and an AP with a 3.5 ms time delay in all three cases. As shown in Fig. 5A and B, however, the same changes in the τ_l resulted in relatively small changes in the peak amplitude, as well as in the overall

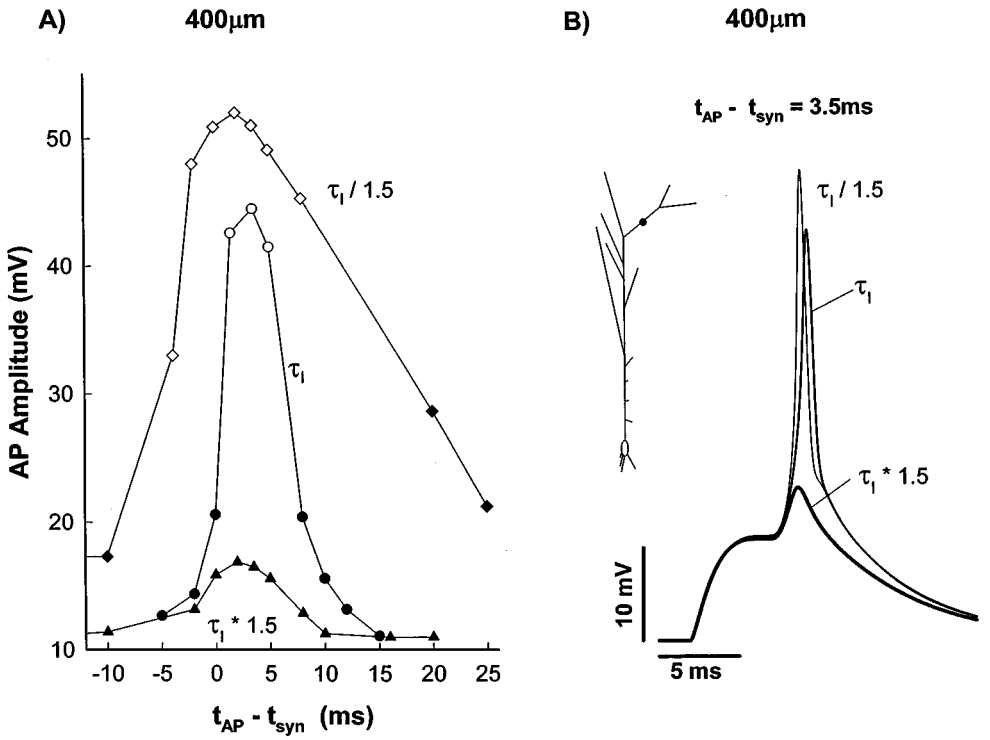

Figure 4. Effect of inactivation rate (τ_l) on pairing AP with synaptic input in distal dendrites. A: AP amplitude at 400 μm from soma, after pairing a synaptic input ($\bar{g}_{\text{esyn}} = 4$ nS) with an AP elicited with different time delays and using different values for τ_l, the time constant of inactivation for $g_{K_A(\text{dist})}$. Open and closed symbols indicate supralinear and sublinear amplification, respectively. B: Membrane potential at the site of synaptic stimulation at 400 μm during a paired activation with an AP elicited at the soma with a 3.5 ms time delay and using different values of τ_l. The black symbol on schematic diagram indicates the location of synaptic stimulation.

shape, of an AP paired with synaptic input at a more proximal (200 μm) location.

In recent experiments the voltage dependence of the $g_{K_A(\text{dist})}$ activation curve was shown to be shifted in a depolarized direction by local protein kinase activity leading to an increased AP amplitude (Hoffman and Johnston, 1998). We tested the effects of a $+5$ mV shift in the $g_{K_A(\text{dist})}$ activation curve on the peak amplitude of a back-propagating AP alone (Fig. 6A) or paired with a synaptic input on a distal dendrite (400 μm, Fig. 6B and C). The reduction in the effects of the $\bar{g}_{K_A(\text{dist})}$ resulted in a more efficient back-propagation of an AP (Fig. 6A, open symbols), in significant changes in the time window for pairing (Fig. 6B, dotted line), and little sensitivity to additional changes in the inactivation time constant (τ_l, Fig. 6C).

Discussion

In this article we have shown how an active dendritic conductance—in particular, a transient K^+ conductance—could modulate the local interaction between a back-propagating AP and a synaptic input. Experiments (Debanne et al., 1998; Magee and Johnston, 1997; Markram et al., 1997; Bi and Poo, 1998) have shown that the pairing of a back-propagating AP with a subthreshold synaptic stimulation can result in either LTP or long-term depression (LTD) of excitatory postsynaptic potentials (EPSPs) depending on the timing. Thus, the back-propagating AP appears to act as a retrograde signal that when paired with synaptic input leads to Hebbian modifications of synaptic strength. The experimental suggestion (Hoffman et al., 1997) that the fast inactivation of a 4-AP dependent K^+ conductance could be a factor in this process is supported by our model, and the findings contribute toward an emerging picture of local associations between back-propagating APs and synaptic input. The optimal coupling was obtained when the AP was elicited 2 to 5 ms after the synaptic stimulation at both 200 and 400 μm from the soma (Fig. 3). It was in the more distal site, however, that the g_{K_A} conductance was shown to strongly

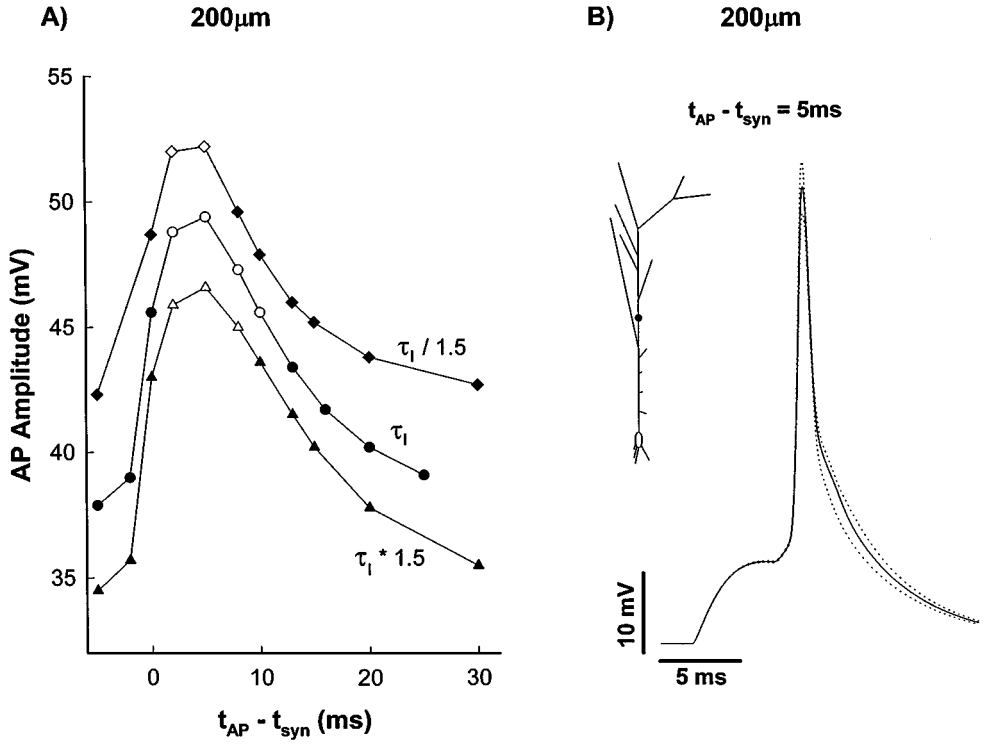

Figure 5. Effect of τ_l on pairing AP with synaptic input in proximal dendrites. A: AP amplitude at 200 μm from soma after pairing a synaptic input ($\bar{g}_{\text{syn}} = 5$ nS) with an AP elicited with different time delays and using different values for τ_l, the time constant of inactivation for $g_{\text{KA(dist)}}$. Open and closed symbols indicate the region of supralinear and sublinear amplification, respectively. B: Membrane potential at the site of synaptic stimulation at 200 μm during a paired activation with an AP elicited at the soma with a 5 ms time delay and using different values of τ_l. The black symbol on schematic diagram indicates the location of synaptic stimulation.

modulate the amount of supralinear amplification of a back-propagating AP. In fact, although both pre- and postsynaptic activity are necessary for Hebbian modifications, the model suggests that the importance of the relative timing for determining LTP or LTD could arise by way of the consequent sub- or supralinear amplification of a back-propagating AP and the resulting Ca^{2+} influx through NMDA receptors or voltage-gated Ca^{2+} channels.

Changes in the activation properties of the g_{KA} conductance, which have been experimentally shown to depend on the local phosphorylation activity (Hoffman and Johnston, 1998, 1999), can modulate APs back-propagating into the dendritic tree. In particular, the model predicts that a small rightward shift in the activation curve could increase the amplitude of a distal dendritic AP (Fig. 6), whereas a change in the time constant of inactivation (cf. Drain et al., 1994; Covarrubias et al., 1994) could alter the time window for a supralinear interaction with a synaptic input (Figs. 3B and 4B).

A number of different and independent dendritic mechanisms appear to have evolved in such a way as to internally limit the back-propagation of single APs and trains of APs. These include the g_{KA} conductance (Hoffman et al., 1997), the slow inactivation of Na^+ channels (Colbert et al., 1997; Jung et al., 1997; Mickus et al., 1999; Migliore and Culotta, 1998; Spruston et al., 1995), and the hyperpolarization-activated (h) channels (Magee, 1998, 1999). The strong depolarization induced by the amplification of back-propagating APs may be an important step for turning on the subcellular mechanisms for new protein synthesis required for long-term change of synaptic strength (Tongiorgi et al., 1997). The inactivation of g_{K_A} with the subsequent increase in AP amplitude would be particularly prominent in the distal portion of the dendritic tree. The effects predicted by our model should be added to the other known roles of g_{K_A} which is countering the effects of NMDA amplification of subthreshold synaptic input in CA1 pyramidal neurons (Cash and Yuste, 1998, 1999) and, more generally, to the amplification

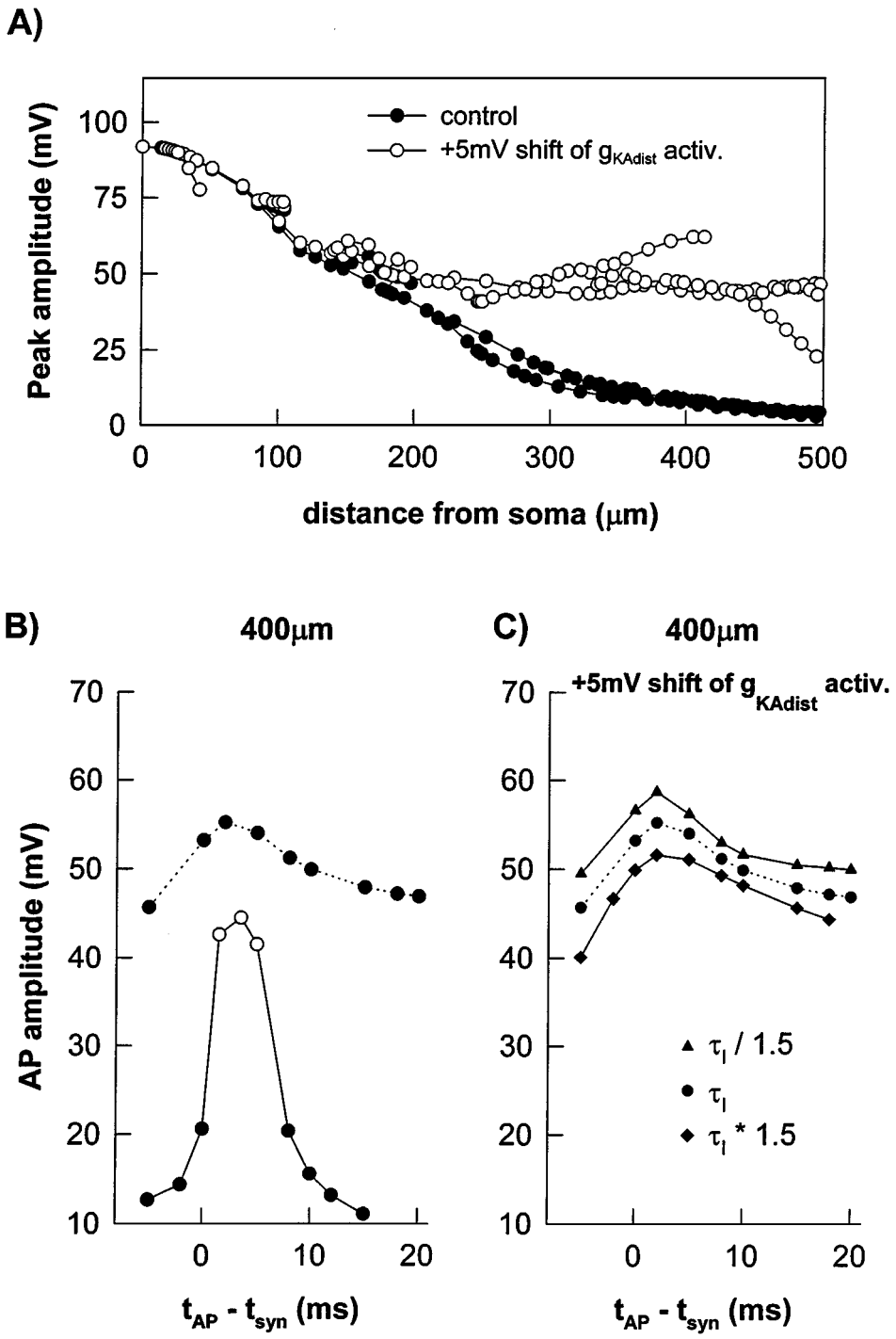

Figure 6. Effects of a +5 mV shift in the $g_{K_A(dist)}$ activation curve. A: Dendritic AP amplitude versus distance from soma in control conditions (closed symbols) and with a +5 mV shift in the $g_{K_A(dist)}$ activation curve (open symbols). A single AP was elicited with a short somatic current pulse (1 nA, 1.2 ms). B: AP amplitude in a compartment at 400 μm from soma, where a synaptic stimulation ($\bar{g}_{syn} = 4$ nS) was paired with a somatic AP in control conditions (solid line) and with a +5 mV shift in the $g_{K_A(dist)}$ activation curve (dotted line). C: AP amplitude at 400 μm from soma showing the effects of changes in the $g_{K_A(dist)}$ inactivation time constant and a +5 mV shift in the activation curve. In panels B and C, open and closed symbols indicate the region of supralinear and sublinear amplification, respectively.

and linearization roles of active conductances in the distal portion of the dendritic tree (Bernander et al., 1994). In different brain regions, such as the visual cortex (Rockland and Virga, 1989) and hippocampus (Johnston and Amaral, 1998), this area of pyramidal neurons receives direct or indirect feedback projections. The elucidation of the membrane characteristics that could modulate such local signals may thus shed light on the operating principles of several brain circuits. In this article, we have shown how the g_{KA} may play a key role in these processes.

Appendix

In the following expressions for the ionic currents, v is in mV, ionic currents are in μA/cm^2, and τ_x (the time constant of a gating variable x) is in ms. A temperature of 35°C was assumed for all simulations.

$$
\begin{aligned}
I_{\mathrm{Na}} &= 32 \cdot m^3 \cdot h \cdot i \cdot (v - 55) \\
m_\infty &= \alpha_m/(\alpha_m + \beta_m); \quad \tau_m = 0.5/(\alpha_m + \beta_m) \\
\alpha_m &= 0.4(v + 30)/(1 - \exp(-(v + 30)/7.2)) \\
\beta_m &= 0.124(v + 30)/(\exp((v + 30)/7.2) - 1) \\
h_\infty &= 1/(1 + \exp((v + 50)/4)) \\
\tau_h &= 0.5/(\alpha_h + \beta_h) \\
\alpha_h &= 0.03(v + 45)/(1 - \exp(-(v + 45)/1.5)) \\
\beta_h &= 0.01(v + 45)/(\exp((v + 45)/1.5) - 1) \\
i_\infty &= (1 + b_i \exp((v + 58)/2))/ \\
&\quad (1 + \exp((v + 58)/2)) \\
\tau_i &= 3 \cdot 10^4 \beta_i \,/(1 + \alpha_i) \\
\alpha_i &= \exp(0.45(v + 60)) \\
\beta_i &= \exp(0.09(v + 60))
\end{aligned}
$$

$b_i = 0.5$ in the apical dendrites, $b_i = 0.8$ in the soma, and $b_i = 1$ elsewhere;

If $\tau_m < 0.02$, then $\tau_m = 0.02$ ms;
If $\tau_h < 0.5$, then $\tau_h = 0.5$ ms;
If $\tau_i < 10$, then $\tau_i = 10$ ms.

$$
\begin{aligned}
I_{\mathrm{K_{DR}}} &= 10 \cdot n \cdot (v + 90) \\
n_\infty &= 1/(1 + \alpha_n); \quad \tau_n = 50\, \beta_n/(1 + \alpha_n) \\
\alpha_n &= \exp(-0.11(v - 13)) \\
\beta_n &= \exp(-0.08(v - 13))
\end{aligned}
$$

If $\tau_n < 2$, then $\tau_n = 2$ ms.

$$
\begin{aligned}
I_{\mathrm{K_{A(prox)}}} &= \bar{g}_{\mathrm{K_{A_p}}} \cdot n \cdot l \cdot (v + 90) \\
\bar{g}_{\mathrm{K_{A_p}}} &= \begin{cases} 48 \cdot (1 + d/100) & \text{for } d \le 100\ \mu\text{m from soma} \\ 0 & \text{for } d > 100\ \mu\text{m from soma} \end{cases} \\
n_\infty &= 1/(1 + \alpha_n); \quad \tau_n = 4\, \beta_n/(1 + \alpha_n) \\
\alpha_n &= \exp(-0.038(1.5 + 1/(1 + \exp(v + 40)/5)) \\
&\quad \cdot (v - 11)) \\
\beta_n &= \exp(-0.038(0.825 + 1/ \\
&\quad (1 + \exp(v + 40)/5)) \cdot (v - 11)) \\
l_\infty &= 1/(1 + \alpha_l); \quad \tau_l = 0.26 \cdot (v + 50) \\
\alpha_l &= \exp(0.11(v + 56))
\end{aligned}
$$

If $\tau_n < 0.1$, then $\tau_n = 0.1$ ms;
If $\tau_l < 2$, then $\tau_l = 2$ ms.

$$
\begin{aligned}
I_{\mathrm{K_{A\,(dist)}}} &= \bar{g}_{\mathrm{K_{A_d}}} \cdot n \cdot l \cdot (v + 90) \\
\bar{g}_{\mathrm{K_{A_d}}} &= \begin{cases} 0 & \text{for } d \le 100\ \mu\text{m from soma} \\ 48 \cdot (1 + d/100) & \text{for } d > 100\ \mu \text{ from soma} \end{cases} \\
n_\infty &= 1/(1 + \alpha_n); \quad \tau_n = 2\, \beta_n/(1 + \alpha_n) \\
\alpha_n &= \exp(-0.038(1.8 + 1/(1 + \exp(v + 40)/5)) \\
&\quad \cdot (v + 1)) \\
\beta_n &= \exp(-0.038(0.7 + 1/(1 + \exp(v + 40)/5)) \\
&\quad \cdot (v + 1)) \\
l_\infty &= 1/(1 + \alpha_l); \quad \tau_l = 0.26 \cdot (v + 50) \\
\alpha_l &= \exp(0.11(v + 56))
\end{aligned}
$$

If $\tau_n < 0.1$, then $\tau_n = 0.1$ ms;
If $\tau_l < 2$, then $\tau_l = 2$ ms.

Acknowledgments

This work was supported in part by the NATO-CNR Senior Fellowship Programme (MM), NIH grants MH44754 and MH48432, the Hankamer Foundation, and the Human Frontiers Science Program (DJ). MM thanks S. Pappalardo for technical assistance.

References

Barrionuevo G, Brown TH (1983) Associative long-term potentiation in hippocampal slices. *Proc. Natl. Acad. Sci. USA* 80:7347–7351.

Bekkers JM, Stevens CF (1990) Computational implications of NMDA receptor channels. *Cold Spring Harb. Symp. Quant. Biol.* 55:131–135.

Bernander Ö, Koch C, Douglas RJ (1994) Amplification and linearization of distal synaptic input to cortical pyramidal cells. *J. Neurophysiol.* 72:2743–2753.

Bi GQ, Poo MM (1998) Synaptic modification in cultured hippocampal neurons: dependence on spike timing, synaptic strength, and postsynaptic cell type. *J. Neurosci.* 18:10464–10472.

Cash S, Yuste R (1998) Input summation by cultured pyramidal neurons is linear and position-independent. *J. Neurosci.* 18:10–15.

Cash S, Yuste R (1999) Linear summation of excitatory inputs by CA1 pyramidal neurons. *Neuron* 22:383–394.

Colbert CM, Johnston D (1996) Axonal action-potential initiation and Na^+ channel densities in the soma and axon initial segment of subicular pyramidal neurons. *J. Neurosci.* 16:6676–6686.

Colbert CM, Johnston D (1998) Protein Kinase C activation decreases activity-dependent attenuation of dendritic Na^+ current in hippocampal CA1 pyramidal neurons. *J. Neurophysiol.* 79:491–495.

Colbert CM, Magee JC, Hoffman DA, Johnston D (1997) Slow recovery from inactivation of Na^+ channels underlie the activity dependent attenuation of dendritic action potentials in hippocampal CA1 pyramidal neurons. *J. Neurosci.* 17:6512–6521.

Covarrubias M, Wei A, Salkoff L, Vyas TB (1994) Elimination of rapid potassium channel inactivation by phosphorylation of the inactivation gate. *Neuron* 13:1403–1412.

Debanne D, Gähwiler BH, Thompson SM (1998) Long-term synaptic plasticity between pairs of individual CA3 pyramidal cells in rat hippocampal slice cultures. *J. Physiol. (Lond.)* 507:237–247.

Drain P, Dubin AE, Aldrich RW (1994) Regulation of *Shaker* K^+ channel inactivation gating by the cAMP-dependent protein kinase. *Neuron* 12:1097–1109.

Gustafsson B, Asztely F, Hanse E, Wigström H (1989) Onset characteristics of long-term potentiation in the guinea-pig hippocampal CA1 region in vitro. *Eur. J. Neurosci.* 1:382–394.

Hines M, Carnevale NT (1997) The NEURON simulation environment. *Neural Comp.* 9:1178–1209.

Hoffman DA, Johnston D (1998) Down-regulation of transient K^+ channels in dendrites of hippocampal CA1 pyramidal neurons by activation of PKA and PKC. *J. Neurosci.* 18:3521–3528.

Hoffman DA, Johnston D (1999) Neuromodulation of dendritic action potentials. *J. Neurophysiol.* 81:408–411.

Hoffman DA, Magee JC, Colbert CM, Johnston D (1997) Potassium channel regulation of signal propagation in dendrites of hippocampal pyramidal neurons. *Nature* 387:869–875.

Holmes WR (1986) Cable theory modeling of the effectiveness of synaptic inputs in cortical pyramidal cells. Ph.D. Thesis, University of California, Los Angeles.

Johnston D, Amaral DG (1998) Hippocampus. In: GM Shepherd, ed. The Synaptic Organization of the Brain, 4th ed. Oxford University Press, New York. pp. 417–458.

Jefferys JG (1975) Propagation of action potentials into the dendrites of hippocampal granule cells in vitro. *J. Physiol. (Lond.)* 249:16P–18P.

Jung H, Mickus T, Spruston N (1997) Prolonged sodium channel inactivation contributes to dendritic action potential attenuation in hippocampal pyramidal neurons. *J. Neurosci.* 17:6639–6646.

Kelso SR, Brown TH (1986) Differential conditioning of associative synaptic enhancement in hippocampal brain slices. *Science* 232:85–87.

Koester HJ, Sakmann B (1998) Calcium dynamics in single spines during coincident pre- and postsynaptic activity depend on relative timing of back-propagating action potentials and subthreshold excitatory postsynaptic potentials. *Proc. Natl. Acad. Sci. USA* 95:9596–9601.

Levy WB, Steward O (1983) Temporal contiguity requirements for long-term associative potentiation/depression in the hippocampus. *Neurosci.* 8:791–797.

Magee, JC (1998) Dendritic hyperpolarization-activated currents modify the integrative properties of hippocampal CA1 pyramidal neurons. *J. Neurosci*.

Magee JC (1999) Dendritic *l-h* normalizes temporal summation in hippocampal CA1 neurons. *Nature Neurosci.* 2:508–514.

Magee JC, Johnston D (1995) Characterization of single voltage gated Na^+ and Ca^{2+} channels in apical dendrites of rat CA1 pyramidal neurons. *J. Physiol.* 487:67–90.

Magee JC, Johnston D (1997) A synaptically controlled, associative signal for Hebbian plasticity in hippocampal neurons. *Science* 275:209–213.

Mainen ZF, Joerges J, Huguenard JR, Sejnowski TJ (1995) A model of spike initiation in neocortical pyramidal neurons. *Neuron* 15:1427–1439.

Markram H, Lübke J, Frotscher M, Sakmann B (1997) Regulation of synaptic efficacy by coincidence of postsynaptic APs and EPSPs. *Science* 275:213–215.

Mickus T, Jung HY, Spruston N (1999) Properties of slow, cumulative sodium channel inactivation in rat hippocampal CA1 pyramidal neurons. *Biophys. J.* 76:846–860.

Migliore M (1996) Modeling the attenuation and failure of action potentials in the dendrites of hippocampal neurons. *Biophys. J.* 71:2394–2403.

Migliore M, Culotta M (1998) Energy efficient modulation of dendritic processing functions. *Biosystems* 48:157–163.

Rapp M, Yarom Y, Segev I (1996) Modeling back propagating action potential in weakly excitable dendrites of neocortical pyramidal cells. *Proc. Natl. Acad. Sci. USA* 93:11985–11990.

Rockland KS, Virga A (1989) Terminal arbors of individual feedback axons projecting from area V2 to V1 in the macaque monkey: A study using immunocitochemistry of anterogradely transported phaseoulus vulgaris-leucoagglutinin. *J. Comp. Neurol.* 285:54–72.

Schiller J, Schiller Y, and Clapham DE (1998). NMDA receptors amplify calcium influx into dendritic spines during associative pre- and postsynaptic activation. *Nature Neurosci.* 1:114–118.

Spruston N, Schiller Y, Stuart G, Sakmann B (1995) Activity-dependent action potential invasion and Ca^{2+} influx into hippocampal CA1 dendrites. *Science* 268:297–300.

Stuart G, Häusser M (1992) Initiation and spread of sodium action potentials in cerebellar Purkinje cells. *Neuron* 13:703–712.

Stuart G, Sakmann B (1994) Active propagation of somatic action potentials into neocortical pyramidal cell dendrites. *Nature* 367:69–72.

Tongiorgi E, Righi M, Cattaneo A (1997) Activity-dependent dendritic targeting of BDNF and TrkB mRNAs in hippocampal neurons. *J. Neurosci.* 17:9492–9505.

Zador A, Koch C, Brown TH (1990) Biophysical model of a Hebbian synapse. *Proc. Natl. Acad. Sci. USA* 87:6718–6722.